Title
Acyl-CoA Dehydrogenase Drives Heat Adaptation by Sequestering Fatty Acids

Journal
Cell, 161(5)

ISSN
0092-8674

Authors
K., Dengke
Li, Zhijie
Lu, Alice Y
et al.

Publication Date
2015-05-01

DOI
10.1016/j.cell.2015.04.026

Peer reviewed

Published in final edited form as:

Cell. 2015 May 21; 161(5): 1152–1163. doi:10.1016/j.cell.2015.04.026.

Acyl-CoA dehydrogenase drives heat adaptation by sequestering fatty acids

Dengke K. Ma[1,*,¶], **Zhijie Li**[2], **Alice Y. Lu**[1], **Fang Sun**[2], **Sidi Chen**[3], **Michael Rothe**[4], **Ralph Menzel**[5], **Fei Sun**[2], and **H. Robert Horvitz**[1,3,*]

[1]Howard Hughes Medical Institute, Department of Biology, McGovern Institute for Brain Research, Massachusetts Institute of Technology, Cambridge, MA 02139, USA

[2]National Laboratory of Biomacromolecules, Institute of Biophysics, Chinese Academy of Sciences, Beijing 100101, China

[3]Koch Institute for Integrative Cancer Research, Massachusetts Institute of Technology, Cambridge, Massachusetts 02139, USA

[4]Lipidomix GmbH, Robert-Roessle-Str. 10, 13125 Berlin, Germany

[5]Freshwater and Stress Ecology, Department of Biology, Humboldt-Universität zu Berlin, Spaethstr. 80/81, 12437 Berlin, Germany

Summary

Cells adapt to temperature shifts by adjusting levels of lipid desaturation and membrane fluidity. This fundamental process occurs in nearly all forms of life, but its mechanism in eukaryotes is unknown. We discovered that the evolutionarily conserved *C. elegans* gene *acdh-11* (acyl-CoA-dehydrogenase, ACDH) facilitates heat adaptation by regulating the lipid desaturase FAT-7. Human ACDH deficiency causes the most common inherited disorders of fatty acid oxidation, with syndromes that are exacerbated by hyperthermia. Heat up-regulates *acdh-11* expression to decrease *fat-7* expression. We solved the high-resolution crystal structure of ACDH-11 and established the molecular basis of its selective and high-affinity binding to C11/C12-chain fatty acids. ACDH-11 sequesters C11/C12-chain fatty acids and prevents these fatty acids from activating nuclear hormone receptors and driving *fat-7* expression. Thus, the ACDH-11 pathway drives heat adaptation by linking temperature shifts to regulation of lipid desaturase levels and membrane fluidity via an unprecedented mode of fatty acid signaling.

*Correspondence: Horvitz@mit.edu or Dengke.Ma@ucsf.edu.

¶Current affiliation: Cardiovascular Research Institute and Department of Physiology, UCSF School of Medicine, San Francisco, California 94158-9001, USA

Author Contributions

H.R.H. supervised the project. D.K.M. initiated the project and with Z.L., A.L., F.S., S.C., M.R., R.M. and F.S. designed and performed the experiments. Z.L. solved the ACDH-11 structures and with F.S. performed the structural analysis. All authors contributed to data analysis, interpretation and manuscript preparation.

Introduction

How cells respond to changes in temperature is a fundamental issue in biology (de Mendoza, 2014; Jordt et al., 2003; Sengupta and Garrity, 2013). Changes in ambient temperature affect nearly all cellular and biochemical processes and drive adaptive responses to maintain cellular homeostasis. For example, up- or down-shifts in temperature increase or decrease the fluidity of the cytoplasmic membrane, respectively. To maintain membrane fluidity within an optimal range for normal biological activity, lipid desaturases in the cell convert saturated fatty acids into unsaturated fatty acids to increase lipid desaturation and thus membrane fluidity in response to temperature downshifts (de Mendoza, 2014; Flowers and Ntambi, 2008; Holthuis and Menon, 2014; Nakamura and Nara, 2004; Zhang and Rock, 2008). Unsaturated double bonds in lipids generate kinks into the otherwise straightened acyl hydrocarbon chain and thereby increase membrane fluidity. This fundamental process of maintaining membrane fluidity is called homeoviscous adaptation (HVA) and occurs in bacteria, archaea, and eukaryotes (Anderson et al., 1981; Cossins and Prosser, 1978; Shmeeda et al., 2002; Sinensky, 1974).

A two-component regulatory system mediates HVA in bacteria (Aguilar et al., 2001; de Mendoza, 2014; Holthuis and Menon, 2014; Zhang and Rock, 2008). In *Bacillus subtilis*, temperature down-shifts induce the expression of the *des* gene, which encodes a lipid desaturase, Des. This induction is controlled by the DesK-DesR two-component system: upon temperature down-shift, the transmembrane histidine kinase DesK phosphorylates and activates the response regulator DesR, which stimulates transcription of *des*. Activation of the DesK-DesR pathway enhances the survival of *Bacillus subtilis* at low temperatures. Whether regulation of lipid desaturation by this pathway is involved in heat adaptation remains unclear. Furthermore, neither DesK nor DesR has apparent homologs in eukaryotes, and specific biological pathways leading to lipid desaturase regulation and HVA in eukaryotes remain unknown.

The nematode *Caenorhabditis elegans* is an ectotherm, i.e. its body temperature depends on external sources. *C. elegans* survives and reproduces optimally over an environmental temperature range of 15°C and 25°C. Temperatures beyond this range cause physiological stress, reduction of fecundity, tissue damage and necrosis (Kourtis et al., 2012; van Oosten-Hawle and Morimoto, 2014). Previous studies of *C. elegans* thermoregulation have focused on understanding how the heat-shock transcription factor HSF-1 functions to maintain proteostasis and cytoskeletal integrity (Baird et al., 2014; van Oosten-Hawle and Morimoto, 2014; van Oosten-Hawle et al., 2013) and on sensory neural circuits and thermotaxis behavioral strategies that allow the animal to navigate a temperature gradient (Garrity et al., 2010; Hedgecock and Russell, 1975; Mori and Ohshima, 1995; Sengupta and Garrity, 2013). Although the *C. elegans* genome encodes seven lipid desaturases that are evolutionarily conserved and involved in fatty acid regulation (Brock et al., 2006; Watts, 2009), the functions and mechanisms of HVA in *C. elegans* have not been explored.

We identified the *C. elegans* gene *acdh-11* (acyl-CoA-dehydrogenase) from a genetic screen exploring how this animal responds to conditions of changing oxygen and subsequently discovered that *acdh-11* functions in HVA and does so by regulating levels of the stearic

Co-A desaturase (SCD) FAT-7. *acdh-11* encodes a member of the evolutionarily conserved ACDH family, which is broadly involved in lipid β-oxidation. To understand the mechanism of action of ACDH-11, we solved its high-resolution crystal structure. This structure helped us establish that ACDH-11 inhibits *fat-7* expression by sequestering C11/C12-chain fatty acids and preventing them from activating *fat-7* expression mediated by the nuclear hormone receptor (NHR) NHR-49, a *C. elegans* homolog of the mammalian fatty acid-binding transcription factors HNF4α and PPARα (Antebi, 2006; Ashrafi, 2007; Atherton et al., 2008; Evans and Mangelsdorf, 2014; Van Gilst et al., 2005). Our findings demonstrate that specific intracellular fatty acids link ACDH-11 in a metabolic pathway to NHRs for transcriptional control of homeoviscous heat adaptation in *C. elegans*. We propose that these molecular principles and mechanisms are evolutionarily conserved and modulate membrane lipid homeostasis and heat adaptation in other organisms.

Results

acdh-11 is required for heat adaptation

We previously reported that the *C. elegans* gene *egl-9* controls a behavioral response to reoxygenation (the O2-ON response) by regulating fatty acid-eicosanoid signaling (Ma et al., 2013; Ma et al., 2012). We examined other *egl* mutants originally isolated based on egg-laying behavioral defects (Trent et al., 1983) and discovered that the previously uncloned gene *egl-25* is also required for both normal egg laying and the O2-ON response (Figures S1A–S1E). We molecularly identified *egl-25* (Figure 1A; Figures S1A–S1E) as the gene *paqr-2* (progestin and adipoQ receptor-2), the sequence of which has similarity to those of mammalian adiponectin receptors and which promotes the adaptation of *C. elegans* to cold temperature (Svensk et al., 2013; Svensson et al., 2011). Since the molecular function of this gene is unclear, we continue to refer to it by its original name, *egl-25*. We confirmed that *egl-25* promotes cold adaptation and the intestinal expression of the SCD gene *fat-7* (Svensk et al., 2013; Svensson et al., 2011) (Figures S1C and S1F).

We expressed a $P_{fat\text{-}7}$*::fat-7::GFP* fluorescent reporter (*nIs590*) in the *egl-25* mutant background to seek *egl-25* suppressor mutations that can restore *fat-7* levels (see Experimental Procedures). We isolated over 40 mutations that suppress *egl-25*, eight of which (*n5655, n5657, n5661, n5876, n5877, n5878, n5879, n5880*) belong to one complementation group and are alleles of a functionally uncharacterized gene named *acdh-11* (Figure 1A). The amino acid sequence of ACDH-11 suggests that it is a long-chain ACDH involved in fatty acid β-oxidation (Ashrafi, 2007; Srinivasan, 2014). *acdh-11* genetically interacts with *acs-3*, which encodes an acyl-CoA synthetase (Ashrafi, 2007; Mullaney et al., 2010). The eight mutations we isolated include one deletion allele and three missense mutations, each of which disrupts an amino acid residue completely conserved among ACDH protein family members (Figure 1B; Figure S2). Such loss-of-function mutations of *acdh-11* restored only slightly the behavioral defects (in egg laying and the O2-ON response) of *egl-25* mutants but caused dramatic up-regulation of $P_{fat\text{-}7}$*::fat-7::GFP* in both *egl-25* mutant and wild-type backgrounds (Figures 1C and 1D).

Because *fat-7* encodes an SCD that catalyzes the limiting step of lipid desaturation and promotes membrane fluidity (de Mendoza, 2014; Flowers and Ntambi, 2008), we monitored

the extent of membrane fluidity in *acdh-11* mutants using the fluorescent dye di-4-ANEPPDHQ (Owen et al., 2012). We found that the fluorescence spectrum of di-4-ANEPPDHQ was red-shifted (Figure S3A), suggesting increased membrane fluidity. Using liquid chromatography-mass spectroscopy (LC-MS) to quantify endogenous levels of various fatty acids, we found that *acdh-11* mutants were abnormal in their compositions of specific fatty acid species (Figure 2A). In particular, we observed a markedly reduced level of stearic acid (C18:0, 18 carbon atoms and 0 double bonds), which is the most abundant saturated fatty acid in *C. elegans* (Figure 2A). The reduced level of C18:0, the metabolic substrate of FAT-7, is consistent with overexpression of $P_{fat\text{-}7}$*::fat-7::GFP* in *acdh-11* mutants. These data indicate that ACDH-11 functions to decrease *fat-7* expression, the desaturation of the FAT-7 substrate stearic acid and membrane lipid fluidity.

Because changes in membrane fluidity are essential for adaptation to temperature shifts, we next examined the temperature sensitivity of *acdh-11* mutants. We found that *acdh-11* mutant embryos successfully developed to adulthood at 15°C or 20°C but failed to do so at 25°C (Figures 2B and 2C). Transgenic expression of wild-type *acdh-11(+)* or decreasing membrane fluidity by supplementing *acdh-11* mutants with the membrane-rigidifying agent dimethyl sulfoxide (DMSO) (Lyman et al., 1976; Sangwan et al., 2001) or reducing the *fat-7* expression level by mutation rescued the 25°C growth defect (Figure 2C). Since temperature higher than 25°C causes heat stress, tissue necrosis and damage in *C. elegans* (Kourtis et al., 2012; van Oosten-Hawle and Morimoto, 2014), we also examined survival of *C. elegans* adults at 37°C and found that *acdh-11* mutants but not *acdh-11*; *fat-7* double mutants exhibited increased death rates compared with wild-type animals (Figure 2D). By contrast, both *acdh-11* mutants and the wild type exhibited similar sensitivity to other types of stress, including high osmolality and oxidative stress (Figures S3B and S3C). These results indicate that ACDH-11 promotes *C. elegans* heat adaptation (also see below) by regulating *fat-7* expression and membrane fluidity.

High temperature up-regulates *acdh-11* expression to decrease *fat-7* expression

We generated a transcriptional reporter strain ($P_{acdh\text{-}11}$*::GFP*) with *GFP* driven by the 0.6 kb promoter of *acdh-11*. We observed that growth at 25°C as opposed to 20°C or 15°C caused marked up-regulation of $P_{acdh\text{-}11}$*::GFP* predominantly in the intestine (Figure 3A), the site of *fat-7* expression, suggesting that ACDH-11 regulates *fat-7* cell-autonomously. Quantitative PCR (qPCR) revealed about a 2-fold induction of endogenous *acdh-11* transcripts at 25°C compared with 15°C (Figure 3B). By contrast, *fat-7* expression in the wild type was strongly decreased at 25°C but increased in *acdh-11* mutants, based upon both RNA-Seq and qPCR experiments (Figures 3C and 3D). This regulation of *fat-7* by *acdh-11* is highly specific to *acdh-11*, since knockdown of *acdh-11* but not of the other 12 members of the *acdh* gene family in *C. elegans* by RNAi caused *fat-7* up-regulation (Figures 3E and 3F). Temperature and *acdh-11* affected *fat-7* expression far more than expression of other *C. elegans fat* genes encoding lipid desaturases, including *fat-5* and *fat-6*, two close *fat-7* homologs in *C. elegans* (Figure 3C) (Murray et al., 2007; Watts, 2009). These results demonstrate up-regulation of *acdh-11* by heat and a highly gene-specific function for *acdh-11* and elevated temperature in regulating the expression of *fat-7*, a member of the

lipid desaturase gene family. These findings are consistent with the hypothesis that *acdh-11* and *fat-7* act in a pathway to facilitate *C. elegans* heat adaptation.

ACDH-11 crystal structure reveals the basis of ACDH-11 interaction with C11/C12-chain fatty acids

To understand the mechanism of action of ACDH-11, we solved its three-dimensional crystal structure as well as its structure in a complex with acyl-CoA (Table S1 and Figure 4). Recombinant *C. elegans* ACDH-11 was expressed from *E. coli*, purified and crystallized (Li et al., 2010). The structure of ACDH-11 was determined by molecular replacement, and the final atomic model of ACDH-11 was refined to 2.27 Å and 1.8 Å resolutions for the apo and the complex structures, respectively (Table S1). The overall structure is tetrameric (Figure 4A), consistent with our previous observation that the purified recombinant ACDH-11 (70 kD momoner) is a 264 kD protein in solution (Li et al., 2010). The monomer has an overall fold similar to that of its two described homologs, the *E. coli* alkylation response protein AidB (Bowles et al., 2008) and the human very long chain acyl-CoA dehydrogenase (VLCAD) (McAndrew et al., 2008). Each ACDH-11 monomer consists of an N-terminal α-helical domain (residues 1–200, α-domain 1), a seven-stranded β-sheet domain (residues 201–320, α-domain 2), a central α-helical domain (residues 321–480, α-domain 3), and a C-terminal α-helical domain (Figure 4B). The tetramer comprises a dimer of dimers, with each subunit providing two loops important for stabilizing the dimer-dimer interaction (Figure 4A; Figures S4A–S4E).

Long-chain ACDHs catalyze the initial step of fatty acid β-oxidation, the dehydrogenation of acyl-CoAs, with substrate-binding pockets that accommodate long-chain fatty acids of varying alkyl chain lengths (Grevengoed et al., 2014). To determine how the interaction of ACDH-11 with its substrates likely impacts HVA, we analyzed the classes of fatty acids that bind to the lipid binding pocket of ACDH-11. We found that ACDH-11 harbored the acyl chain of the fatty acid C11-CoA as a ligand in the crystal (Figure 4C; Figures 5A–5E). C11-CoA was deeply buried inside a 14 Å-depth binding cavity of ACDH-11, the depth of which was restricted by two residues, Tyr 344 and Leu 159, limiting the maximum carbon length to C12 (Figure 4C; Figure 5A). The temperature B-factors (Woldeyes et al., 2014), which indicate the motilities of these two amino acids (Tyr 344 and Leu 159), are relatively low across the entire ACDH-11 sequence (Figure 5B). The ligand-free apo-structure of ACDH-11 displays the same conformation of Tyr 344 and Leu 159 (Figures S5C and S5D), further supporting the conclusion that the size of the binding cavity would not accommodate fatty acid carbon lengths longer than C12.

The structure reveals that strong binding of ACDH-11 to C11-CoA is mediated by at least ten hydrogen bond interactions (Figure 5A), including one between Ser 267 and the 3'-phosphate on the CoA moiety; two between the side chain of Asn 331 and the N2 and N3 nitrogens of the adenine ring; two between the side chain of Arg 321 and the O4 and O5 oxygens in the adenosine 3', 5'-diphosphate group; two between the side chain of Arg 476 and the O9 and O10 oxygens of the pyrophosphate portion; two between the side chain of Arg334 and the O1 and O2 oxygens of the peptidyl portion; and one between the main chain of Ser215 and the N2 nitrogen of the peptidyl portion. We compared the structure of

ACDH11 bound with C11-CoA with other structurally characterized ACDHs (SCAD, MCAD and VLCAD) (Battaile et al., 2002; Kim et al., 1993; McAndrew et al., 2008) and found that ACDH-11 provides more hydrogen bonds (Figure S6) than other ACDHs and binds to the acyl chain via hydrophobic interactions that are defined by a deep binding pocket (Figure 5A). Using isothermal titration calorimetry (ITC), we quantified the binding affinities of C12-CoA and C8, C10, C12 fatty acids (we tested these even number chain-fatty acids, since their synthetic forms are readily available) to purified ACDH-11. The ITC results (Figures 5C–5E) showed that the disassociation constants for C10, C12 and C12-CoA binding to purified ACDH-11 are 21.3±2.6 μM, 10.3±2.4 μM and 5.2±1.3 μM, respectively, and no significant binding was detected for C8 (Figures S5G and S5H). These biochemical results demonstrate the selectivity of ACDH-11 for fatty acids with chain lengths from C10 to C12, fully consistent with our conclusions based on structural observations. We obtained the structure of the complex without having added any ligand supplement during crystal growth, as C11-CoA presumably was tightly sequestered by ACDH-11 during the step of protein expression in *E. coli*.

ACDH-11, C11/C12-fatty acids and NHR-49 act in a pathway to drive heat adaptation

The strong and selective binding of C11/C12-chain fatty acids to ACDH-11 indicated by the crystal structure of ACDH-11 could explain the functional specificity of ACDH-11 in regulating *fat-7* expression and heat adaptation. Specifically, we hypothesize that heat-induced ACDH-11 sequesters intracellular C11/C12-chain fatty acids, which are required for activating nuclear *fat-7* expression through fatty acid-regulated transcription factors.

To test this hypothesis, we examined whether supplementing *C. elegans* with exogenous fatty acids of various lengths could stimulate *fat-7* expression. We tested effects of a fatty acid series from C3 to C20 on the expression of $P_{fat\text{-}7}$*::fat-7::GFP*. At 25°C, this reporter was turned off (Figure 6A). Most of the fatty acids had no significant effects on FAT-7::GFP expression. By contrast, C10, C11, and C12 activated reporter expression in markedly higher fractions of the animals (Figure 6A). The activity of C10 was lower than that of C11 and C12. *fat-7* is a known transcriptional target of NHR-49 (Pathare et al., 2012; Van Gilst et al., 2005), a *C. elegans* homolog of the mammalian transcription factors PPARα and HNF4α, which are known to bind fatty acids, including C12 (Dhe-Paganon et al., 2002). We found that *nhr-49* RNAi eliminated the effect of C11 or C12 in activating FAT-7::GFP (Figure 6B). *nhr-49* RNAi or mutations also completely blocked overexpression of FAT-7::GFP in *acdh-11* mutants (Figure 6B and Figure S7A). NHR-49 shares high sequence identity (37% amino acid residues, Figures S7B and S7C) with HNF4α (Dhe-Paganon et al., 2002), suggesting that NHR-49 likely exhibits a fatty acid-binding pocket that can accommodate C11/C12 fatty acids. These results indicate that C11/C12 requires NHR-49 to activate *fat-7* expression and that ACDH-11 sequesters C11/C12 fatty acids and thereby prevents them from activating nuclear *fat-7* expression.

Discussion

Based on our observations, we propose a model for how ACDH-11 regulates *C. elegans* heat adaptation (Figure 7). Under cold conditions (e.g. 15°C), intracellular C11/C12 fatty acids

promote *fat-7* expression via fatty acid-regulated nuclear receptors (e.g. NHR-49). Up-regulation of *fat-7* promotes lipid desaturation and thus membrane fluidity, which is an adaptation to cold. As a PAQR-related transmembrane protein with a ceramidase or phospholipase-like domain (Pei et al., 2011), EGL-25 likely acts to increase levels of C11/C12 and hence promote signaling in cooperation with NHR-49 (Svensk et al., 2013) and other NHRs (Brock et al., 2006; Pathare et al., 2012) for cold adaptation. Our data suggest that intracellular C11/C12 fatty acids activate *fat-7* expression via NHRs, which likely require lipid-transporting proteins to transduce C11/C12 fatty acid signals into the nucleus; however, we do not exclude the possibility that C11/C12 fatty acids might be further metabolized or processed to indirectly modulate NHR activation. In the cold, *acdh-11* is expressed at low levels and has little or no function.

Under heat conditions (e.g. 25°C), *acdh-11* is transcriptionally up-regulated, and elevated levels of the ACDH-11 protein sequester intracellular C11/C12, preventing downstream NHR activation and consequent *fat-7* expression, thereby promoting lipid saturation and membrane rigidity in response to heat. Upstream sensors and mediators of this heat-induced *acdh-11* up-regulation remain to be identified. At high temperature, in both wild-type animals and *egl-25* mutants C11/C12 is sequestered by ACDH-11, resulting in normal adaption to heat. By contrast, in *egl-25*; *acdh-11* double mutants as well as in *acdh-11* single mutants, C11/C12 is not sequestered by ACDH-11 and its consequent higher levels drive *fat-7* expression (although *fat-7* expression requires NHR-49, our data do not preclude the possibility that ACDH-11 sequestration of C11/C12 also prevents the activation of other NHRs). The resulting membrane lipid desaturation causes excessive membrane fluidity and thus a failure to adapt to heat. The genetic epistatic interactions among *egl-25, acdh-11* and *nhr-49*, the high penetrance of their corresponding mutant phenotypes (Figure 1 and Figure S7A) as well as mechanistic insights from the ACDH-11 structure together strongly support this model.

In both prokaryotic and eukaryotic cells, SCD fatty acid desaturases catalyze the limiting step of fatty acid desaturation and mediate HVA by maintaining optimal ranges of membrane fluidity in response to temperature shifts (Cossins and Prosser, 1978; de Mendoza, 2014; Flowers and Ntambi, 2008; Sinensky, 1974; Zhang and Rock, 2008). Bacterial two-component systems, which are not present in eukaryotes, link membrane sensing of temperature shifts to nuclear transcription of desaturase genes for HVA (Aguilar et al., 2001; de Mendoza, 2014). Eukaryotic organisms, including warm-blooded animals, also exhibit HVA (Anderson et al., 1981; Cossins and Prosser, 1978; Shmeeda et al., 2002), a phenomenon far less studied and understood than bacterial HVA. Unlike systemic thermoregulation, eukaryotic HVA likely evolved as a mechanism to locally and cell-autonomously respond to temperature shifts. Cold temperature up-regulates plasma levels of adiponectin in humans (Imbeault et al., 2009), although roles of adiponectin and its receptors in HVA have not been explored. *C. elegans* SCDs and adiponectin receptor homologs have been proposed to regulate cold adaptation (Svensk et al., 2013; Svensson et al., 2011). Our findings support this hypothesis and further identify functional roles of ACDH-11 and C11/C12 fatty acids in the *egl-25* and *fat-7* pathway to control HVA in *C. elegans*. Unlike long-chain fatty acids that are well-known to mediate various cell signaling

processes, sequestration of medium-chain C11/C12 fatty acids by ACDH-11 represents an unprecedented mode of fatty acid signaling. The novel pathway and mechanisms we have discovered provide a molecular basis for homeoviscous heat adaptation in *C. elegans*, shedding light on a long-standing mystery concerning a fundamental cell biological problem.

Mutations in human ACDH genes cause disorders of fatty acid oxidation that become life-threatening under fever or hyperthermia (Jank et al., 2014; O'Reilly et al., 2004; Zolkipli et al., 2011), with responses that are analogous to the vulnerability of *C. elegans acdh-11* mutants to heat. Although maintaining a sufficient diet is currently the standard-of-care management option to prevent symptoms of ACDH-deficiency in human patients, hyperthermia is a more significant independent risk factor than hypoglycemia (Rinaldo et al., 2002; Wolfe et al., 1993; Zolkipli et al., 2011). Our findings suggest that imbalance of lipid desaturation contributes to heat sensitivity of human ACDH-deficient patients and that therapeutic targeting of lipid desaturases might alleviate the thermo-sensitive syndrome of human ACDH-deficient patients. In addition, we found that ACDH-11 acts in a metabolic pathway to modulate activation of nuclear receptors by sequestering C11/C12 fatty acids, a plausibly widespread mechanism of controlling intracellular fatty acid signaling. Given that lipid metabolism and signaling are fundamentally similar between nematodes and other organisms (Ashrafi, 2007; Grevengoed et al., 2014; Holthuis and Menon, 2014; McKay et al., 2003; Nakamura and Nara, 2004; Srinivasan, 2014; Watts, 2009), we propose that the pathway and mechanisms we have identified for *C. elegans* are evolutionarily conserved and modulate lipid metabolic homeostasis as well as thermal adaptation-associated physiological and pathological processes in other organisms, including humans.

Experimental Procedures

EMS mutagenesis, genetic screens and whole-genome sequencing

To screen for *egl-25* suppressors, we mutagenized *egl-25(n573)* mutants carrying the $P_{fat\text{-}7}$*::fat-7::GFP* transgene *nIs590* with ethyl methanesulfonate (EMS) and observed the F2 progeny using a dissecting microscope and GFP fluorescence at 20°C. We isolated suppressor mutants with restored expression of $P_{fat\text{-}7}$*::fat-7::GFP* in *egl-25* mutants. We mapped the suppressor mutations using standard genetic techniques based on polymorphic SNPs between the Bristol strain N2 and the Hawaiian strain CB4856 (Davis et al., 2005). We used whole-genome sequencing to identify the mutations; data analyses were performed as described (Sarin et al., 2008).

Mutations and Strains

C. elegans strains were cultured as described (Brenner, 1974). The N2 Bristol strain (Brenner, 1974) was the reference wild-type strain, and the polymorphic Hawaiian strain CB4856 (Wicks et al., 2001) was used for genetic mapping and SNP analysis. Mutations used were as follows: LG I, *nhr-49(nr2041)* (Van Gilst et al., 2005); LG III, *egl-25(n573, gk395168, ok3136)* (Thompson et al., 2013b; Trent et al., 1983), *acdh-11(n5655, n5657, n5661, n5876, n5877, n5878, n5879, n5880, gk753061);* LG V, *fat-7(wa36)* (Watts and Browse, 2000). *gk395168* and *gk753061* (molecular null, causing an L119-to-amber stop

codon) were obtained from the Million Mutation Project and outcrossed six times (Thompson et al., 2013a).

Transgenic strains were generated by germline transformation (Mello et al., 1991). Transgenic constructs were co-injected (at 10 – 50 ng/μl) with mCherry reporters, and lines of mCherry-positive animals were established. Gamma irradiation was used to generate integrated transgenes. Transgenic strains used were as follows: *nIs590[P_{fat-7}::fat-7::GFP]* (integrated from the extrachromosomal array *waEx15[P_{fat-7}::GFP + lin15(+)]* (Brock et al., 2006)); *nIs616[egl-25(+); P_{unc-54}::mCherry]; nIs677[$P_{acdh-11}$::GFP; P_{unc-54}::mCherry]; nEx2270[acdh-11(+);P_{unc-54}::mCherry]*.

Protein purification, structure determination, model building and refinement

Protein was expressed and purified as described (Li et al., 2010). Briefly, the *acdh-11* gene was amplified and cloned into the expression vector pEXS-DH (derived from pET-22b, Novagen). 8xHis-tagged ACDH-11 was expressed in the *E. coli* strain BL21 (DE3) and isolated from the cell lysate by Ni2+-NTA (Qiagen) affinity chromatography. ACDH-11 was further purified using ion exchange chromatography (RESOURCE S column, GE Healthcare) and size exclusion chromatography (Superdex 200 100/300 GL Column, GE Healthcare). For crystallization, ACDH-11 was concentrated to 12 mg/ml in 20 mM Tris pH 8.0, 150 mM NaCl. Large yellow crystals grew in 100 mM Tris pH 8.0, 200 mM magnesium formate and 13% PEG 3350 through sitting-drop vapor diffusion at 16°C.

Immediately prior to data collection, the ACDH-11 crystal was quickly soaked in cryoprotectant solution (13% PEG 3350 and 20% glycerol) and flash-cooled at 100°K in a stream of nitrogen gas. The high-resolution diffraction data set for the complex structure was collected on beamline BL5A of the Photon Factory (KEK, Japan). The diffraction data set for the apo structure was collected on beamline BL17U of Shanghai Synchrotron Radiation Facility (SSRF, China). The structure of ACDH-11 was resolved by molecular replacement using the program Phaser (McCoy et al., 2007). ACDH-11 shares 30% sequence identity with *E. coli* AidB (Bowles et al., 2008), and the refined coordinates of AidB were used to construct the search model. The programs Coot (Emsley and Cowtan, 2004) and Refmac5 (Murshudov et al., 1997) were used for manual model building and refinement. The difference-Fourier map exhibited long and continuous electron densities corresponding to the FAD co-factor acyl-CoA. The length of acyl-chain was determined according to the electron density. C11-CoA was assigned because of its best RSCC (real space correlation coefficient, see Figures 5E and 5F). The statistics of data collection and structural refinement are summarized in Table S1.

The coordinates for the final refined model were deposited in PDB (protein data bank) with the accession number 4Y9J for the C11-CoA bound structure and 4Y9L for the C11-CoA free structure of ACDH-11.

Isothermal titration calorimetry

Isothermal titration calorimetry (ITC) measurements were performed with a MicroCal iTC-200 titration micro-calorimeter (GE Healthcare, MA, USA) at 25 °C. The sample cell

was filled with ACDH-11 (25μM in 20 mM MES, pH 6.5 and 10% glycerol). ACDH-11 concentration was determined by the BCA (Bicinchoninic Acid) method. The free fatty acids C8, C10, C12 and C14, and C12-CoA (800 μM) prepared in the same buffer were injected into the sample cell in 2-minute time intervals. 20 injections in total were conducted within 40 min. The reaction solution contained 1% DMSO to increase the solubility of fatty acids. As negative control, the ligands were titrated into the buffer without ACDH-11 proteins. All experiments were repeated five times. The data were processed using the Origin software (Version 7.0).

Gene expression analyses

For qPCR and RNA-Seq experiments, total RNA from age-synchronized young adult (24 hrs post-L4) hermaphrodites (200 in total, picked manually) was prepared using TissueRuptor and the RNeasy Mini kit (Qiagen). Reverse transcription was performed by SuperScript III, and quantitative PCR was performed using Applied Biosystems Real-Time PCR Instruments. The specific intron-spanning primer sequences used were: *act-3* forward – TCCATCATGAAGTGCGACAT; *act-3* reverse – TAGATCCTCCGATCCAGACG; *fat-7* forward – ACGAGCTTGTCTTCCATGCT; *fat-7* reverse – AGCCCATTCAATGATGTCGT; *acdh-11* forward – TTGATCCATTTGTTCGGAGA; *acdh-11* reverse – GGTGGCTAGCTTGTGCTTTC. RNA-Seq was performed by the Illumina TruSeq chemistry, and data were analyzed using standard protocols (Trapnell et al., 2010).

Nomarski and GFP fluorescence images of anesthetized *C. elegans* were obtained using an Axioskop II (Zeiss) compound microscope and OpenLab software (Agilent). The fraction of FAT-7::GFP-positive animals observed was quantified by counting animals using a dissecting microscope equipped for the detection of GFP fluorescence.

Supplementary Material

Refer to Web version on PubMed Central for supplementary material.

Acknowledgements

We thank E. Boyden, A. Fire, Y. Iino and M. Pilon for reagents and the *Caenorhabditis* Genetics Center and the Million Mutation Project for strains. M. Bai, N. Bhatla, S. Luo, R. Vozdek, T. Wang and J. Ward for comments on the manuscript. H.R.H. is an Investigator of the Howard Hughes Medical Institute and the David H. Koch Professor of Biology at MIT. This work was supported by NIH grants GM24663 (H.R.H.), K99HL116654 (D.K.M.), Chinese Ministry of Science and Technology grant 2011CB910301 and 2011CB910901 (F.S.), German Research Foundation grant ME2056/3-1 (R.M.), Damon Runyon Fellowship DRG-2117-12 (S.C.) and Helen Hay Whitney and Charles King Trust postdoctoral fellowships (D.K.M.).

References

Aguilar PS, Hernandez-Arriaga AM, Cybulski LE, Erazo AC, de Mendoza D. Molecular basis of thermosensing: a two-component signal transduction thermometer in *Bacillus subtilis*. EMBO J. 2001; 20:1681–1691. [PubMed: 11285232]

Anderson RL, Minton KW, Li GC, Hahn GM. Temperature-induced homeoviscous adaptation of Chinese hamster ovary cells. Biochim Biophys Acta. 1981; 641:334–348. [PubMed: 7213723]

Antebi A. Nuclear hormone receptors in *C. elegans*. WormBook. 2006:1–13. [PubMed: 18050471]

Ashrafi K. Obesity and the regulation of fat metabolism. WormBook. 2007:1–20. [PubMed: 18050496]

Atherton HJ, Jones OA, Malik S, Miska EA, Griffin JL. A comparative metabolomic study of NHR-49 in *Caenorhabditis elegans* and PPAR-alpha in the mouse. FEBS Lett. 2008; 582:1661–1666. [PubMed: 18435929]

Baird NA, Douglas PM, Simic MS, Grant AR, Moresco JJ, Wolff SC, Yates JR 3rd, Manning G, Dillin A. HSF-1-mediated cytoskeletal integrity determines thermotolerance and life span. Science. 2014; 346:360–363. [PubMed: 25324391]

Battaile KP, Molin-Case J, Paschke R, Wang M, Bennett D, Vockley J, Kim JJ. Crystal structure of rat short chain acyl-CoA dehydrogenase complexed with acetoacetyl-CoA: comparison with other acyl-CoA dehydrogenases. J Biol Chem. 2002; 277:12200–12207. [PubMed: 11812788]

Bowles T, Metz AH, O'Quin J, Wawrzak Z, Eichman BF. Structure and DNA binding of alkylation response protein AidB. Proc Natl Acad Sci U S A. 2008; 105:15299–15304. [PubMed: 18829440]

Brenner S. The genetics of *Caenorhabditis elegans*. Genetics. 1974; 77:71–94. [PubMed: 4366476]

Brock TJ, Browse J, Watts JL. Genetic regulation of unsaturated fatty acid composition in *C. elegans*. PLoS Genet. 2006; 2:e108. [PubMed: 16839188]

Cossins AR, Prosser CL. Evolutionary adaptation of membranes to temperature. Proc Natl Acad Sci U S A. 1978; 75:2040–2043. [PubMed: 273929]

Davis MW, Hammarlund M, Harrach T, Hullett P, Olsen S, Jorgensen EM. Rapid single nucleotide polymorphism mapping in *C. elegans*. BMC Genomics. 2005; 6 10.1186/1471-2164-1186-1118.

de Mendoza D. Temperature Sensing by Membranes. Annu Rev Microbiol. 2014

Dhe-Paganon S, Duda K, Iwamoto M, Chi YI, Shoelson SE. Crystal structure of the HNF4 alpha ligand binding domain in complex with endogenous fatty acid ligand. J Biol Chem. 2002; 277:37973–37976. [PubMed: 12193589]

Emsley P, Cowtan K. Coot: model-building tools for molecular graphics. Acta Crystallogr D Biol Crystallogr. 2004; 60:2126–2132. [PubMed: 15572765]

Evans RM, Mangelsdorf DJ. Nuclear Receptors, RXR, and the Big Bang. Cell. 2014; 157:255–266. [PubMed: 24679540]

Flowers MT, Ntambi JM. Role of stearoyl-coenzyme A desaturase in regulating lipid metabolism. Curr Opin Lipidol. 2008; 19:248–256. [PubMed: 18460915]

Garrity PA, Goodman MB, Samuel AD, Sengupta P. Running hot and cold: behavioral strategies, neural circuits, and the molecular machinery for thermotaxis in *C. elegans* and Drosophila. Genes Dev. 2010; 24:2365–2382. [PubMed: 21041406]

Grevengoed TJ, Klett EL, Coleman RA. Acyl-CoA Metabolism and Partitioning. Annu Rev Nutr. 2014; 34:1–30. [PubMed: 24819326]

Hedgecock EM, Russell RL. Normal and mutant thermotaxis in the nematode *Caenorhabditis elegans*. Proc Natl Acad Sci U S A. 1975; 72:4061–4065. [PubMed: 1060088]

Holthuis JC, Menon AK. Lipid landscapes and pipelines in membrane homeostasis. Nature. 2014; 510:48–57. [PubMed: 24899304]

Imbeault P, Depault I, Haman F. Cold exposure increases adiponectin levels in men. Metabolism. 2009; 58:552–559. [PubMed: 19303978]

Jank JM, Maier EM, Reibeta DD, Haslbeck M, Kemter KF, Truger MS, Sommerhoff CP, Ferdinandusse S, Wanders RJ, Gersting SW, et al. The domain-specific and temperature-dependent protein misfolding phenotype of variant medium-chain acyl-CoA dehydrogenase. PLoS One. 2014; 9:e93852. [PubMed: 24718418]

Jordt SE, McKemy DD, Julius D. Lessons from peppers and peppermint: the molecular logic of thermosensation. Curr Opin Neurobiol. 2003; 13:487–492. [PubMed: 12965298]

Kim JJ, Wang M, Paschke R. Crystal structures of medium-chain acyl-CoA dehydrogenase from pig liver mitochondria with and without substrate. Proc Natl Acad Sci U S A. 1993; 90:7523–7527. [PubMed: 8356049]

Kourtis N, Nikoletopoulou V, Tavernarakis N. Small heat-shock proteins protect from heat-stroke-associated neurodegeneration. Nature. 2012; 490:213–218. [PubMed: 22972192]

Li Z, Zhai Y, Fang J, Zhou Q, Geng Y, Sun F. Purification, crystallization and preliminary crystallographic analysis of very-long-chain acyl-CoA dehydrogenase from *Caenorhabditis elegans*. Acta Crystallogr Sect F Struct Biol Cryst Commun. 2010; 66:426–430.

Lyman GH, Preisler HD, Papahadjopoulos D. Membrane action of DMSO and other chemical inducers of Friend leukaemic cell differentiation. Nature. 1976; 262:361–363. [PubMed: 986559]

Ma DK, Rothe M, Zheng S, Bhatla N, Pender CL, Menzel R, Horvitz HR. Cytochrome P450 drives a HIF-regulated behavioral response to reoxygenation by *C. elegans*. Science. 2013; 341:554–558. [PubMed: 23811225]

Ma DK, Vozdek R, Bhatla N, Horvitz HR. CYSL-1 interacts with the O2-sensing hydroxylase EGL-9 to promote H2S-modulated hypoxia-induced behavioral plasticity in C. elegans. Neuron. 2012; 73:925–940. [PubMed: 22405203]

McAndrew RP, Wang Y, Mohsen AW, He M, Vockley J, Kim JJ. Structural basis for substrate fatty acyl chain specificity: crystal structure of human very-long-chain acyl-CoA dehydrogenase. J Biol Chem. 2008; 283:9435–9443. [PubMed: 18227065]

McCoy AJ, Grosse-Kunstleve RW, Adams PD, Winn MD, Storoni LC, Read RJ. Phaser crystallographic software. J Appl Crystallogr. 2007; 40:658–674. [PubMed: 19461840]

McKay RM, McKay JP, Avery L, Graff JM. *C elegans*: a model for exploring the genetics of fat storage. Dev Cell. 2003; 4:131–142. [PubMed: 12530969]

Mello CC, Kramer JM, Stinchcomb D, Ambros V. Efficient gene transfer in *C. elegans*: extrachromosomal maintenance and integration of transforming sequences. EMBO J. 1991; 10:3959–3970. [PubMed: 1935914]

Mori I, Ohshima Y. Neural regulation of thermotaxis in *Caenorhabditis elegans*. Nature. 1995; 376:344–348. [PubMed: 7630402]

Mullaney BC, Blind RD, Lemieux GA, Perez CL, Elle IC, Faergeman NJ, Van Gilst MR, Ingraham HA, Ashrafi K. Regulation of *C. elegans* fat uptake and storage by acyl-CoA synthase-3 is dependent on NR5A family nuclear hormone receptor nhr-25. Cell Metab. 2010; 12:398–410. [PubMed: 20889131]

Murray P, Hayward SA, Govan GG, Gracey AY, Cossins AR. An explicit test of the phospholipid saturation hypothesis of acquired cold tolerance in *Caenorhabditis elegans*. Proc Natl Acad Sci U S A. 2007; 104:5489–5494. [PubMed: 17369360]

Murshudov GN, Vagin AA, Dodson EJ. Refinement of macromolecular structures by the maximum-likelihood method. Acta Crystallogr D Biol Crystallogr. 1997; 53:240–255. [PubMed: 15299926]

Nakamura MT, Nara TY. Structure, function, and dietary regulation of delta6, delta5, and delta9 desaturases. Annu Rev Nutr. 2004; 24:345–376. [PubMed: 15189125]

O'Reilly L, Bross P, Corydon TJ, Olpin SE, Hansen J, Kenney JM, McCandless SE, Frazier DM, Winter V, Gregersen N, et al. The Y42H mutation in medium-chain acyl-CoA dehydrogenase, which is prevalent in babies identified by MS/MS-based newborn screening, is temperature sensitive. Eur J Biochem. 2004; 271:4053–4063. [PubMed: 15479234]

Owen DM, Rentero C, Magenau A, Abu-Siniyeh A, Gaus K. Quantitative imaging of membrane lipid order in cells and organisms. Nat Protoc. 2012; 7:24–35. [PubMed: 22157973]

Pathare PP, Lin A, Bornfeldt KE, Taubert S, Van Gilst MR. Coordinate regulation of lipid metabolism by novel nuclear receptor partnerships. PLoS Genet. 2012; 8:e1002645. [PubMed: 22511885]

Pei J, Millay DP, Olson EN, Grishin NV. CREST--a large and diverse superfamily of putative transmembrane hydrolases. Biol Direct. 2011; 6:37. [PubMed: 21733186]

Rinaldo P, Matern D, Bennett MJ. Fatty acid oxidation disorders. Annu Rev Physiol. 2002; 64:477–502. [PubMed: 11826276]

Sangwan V, Foulds I, Singh J, Dhindsa RS. Cold-activation of Brassica napus BN115 promoter is mediated by structural changes in membranes and cytoskeleton, and requires Ca2+ influx. Plant J. 2001; 27:1–12. [PubMed: 11489178]

Sarin S, Prabhu S, O'Meara MM, Pe'er I, Hobert O. *Caenorhabditis elegans* mutant allele identification by whole-genome sequencing. Nat Methods. 2008; 5:865–867. [PubMed: 18677319]

Sengupta P, Garrity P. Sensing temperature. Curr Biol. 2013; 23:R304–R307. [PubMed: 23618661]

Shmeeda H, Kaspler P, Shleyer J, Honen R, Horowitz M, Barenholz Y. Heat acclimation in rats: modulation via lipid polyunsaturation. Am J Physiol Regul Integr Comp Physiol. 2002; 283:R389–R399. [PubMed: 12121852]

Sinensky M. Homeoviscous adaptation--a homeostatic process that regulates the viscosity of membrane lipids in *Escherichia coli*. Proc Natl Acad Sci U S A. 1974; 71:522–525. [PubMed: 4360948]

Srinivasan S. Regulation of Body Fat in *Caenorhabditis elegans*. Annu Rev Physiol. 2014

Svensk E, Stahlman M, Andersson CH, Johansson M, Boren J, Pilon M. PAQR-2 regulates fatty acid desaturation during cold adaptation in *C. elegans*. PLoS Genet. 2013; 9:e1003801. [PubMed: 24068966]

Svensson E, Olsen L, Morck C, Brackmann C, Enejder A, Faergeman NJ, Pilon M. The adiponectin receptor homologs in *C. elegans* promote energy utilization and homeostasis. PLoS One. 2011; 6:e21343. [PubMed: 21712952]

Thompson O, Edgley M, Strasbourger P, Flibotte S, Ewing B, Adair R, Au V, Chaudhry I, Fernando L, Hutter H, et al. The million mutation project: a new approach to genetics in *Caenorhabditis elegans*. Genome Res. 2013a; 23:1749–1762. [PubMed: 23800452]

Thompson O, Edgley M, Strasbourger P, Flibotte S, Ewing B, Adair R, Au V, Chaudry I, Fernando L, Hutter H, et al. The Million Mutation Project: A new approach to genetics in *Caenorhabditis elegans*. Genome Res. 2013b

Trapnell C, Williams BA, Pertea G, Mortazavi A, Kwan G, van Baren MJ, Salzberg SL, Wold BJ, Pachter L. Transcript assembly and quantification by RNA-Seq reveals unannotated transcripts and isoform switching during cell differentiation. Nat Biotechnol. 2010; 28:511–515. [PubMed: 20436464]

Trent C, Tsung N, Horvitz HR. Egg-laying defective mutants of the nematode *Caenorhabditis elegans*. Genetics. 1983; 104:619–647. [PubMed: 11813735]

Van Gilst MR, Hadjivassiliou H, Jolly A, Yamamoto KR. Nuclear hormone receptor NHR-49 controls fat consumption and fatty acid composition in *C. elegans*. PLoS Biol. 2005; 3:e53. [PubMed: 15719061]

van Oosten-Hawle P, Morimoto RI. Organismal proteostasis: role of cell-nonautonomous regulation and transcellular chaperone signaling. Genes Dev. 2014; 28:1533–1543. [PubMed: 25030693]

van Oosten-Hawle P, Porter RS, Morimoto RI. Regulation of organismal proteostasis by transcellular chaperone signaling. Cell. 2013; 153:1366–1378. [PubMed: 23746847]

Watts JL. Fat synthesis and adiposity regulation in *Caenorhabditis elegans*. Trends Endocrinol Metab. 2009; 20:58–65. [PubMed: 19181539]

Watts JL, Browse J. A palmitoyl-CoA-specific delta9 fatty acid desaturase from *Caenorhabditis elegans*. Biochem Biophys Res Commun. 2000; 272:263–269. [PubMed: 10872837]

Wicks SR, Yeh RT, Gish WR, Waterston RH, Plasterk RH. Rapid gene mapping in *Caenorhabditis elegans* using a high density polymorphism map. Nat Genet. 2001; 28:160–164. [PubMed: 11381264]

Woldeyes RA, Sivak DA, Fraser JS. E pluribus unum, no more: from one crystal, many conformations. Curr Opin Struct Biol. 2014; 28C:56–62. [PubMed: 25113271]

Wolfe L, Jethva R, Oglesbee D, Vockley J. Short-Chain Acyl-CoA Dehydrogenase Deficiency. 1993

Zhang YM, Rock CO. Membrane lipid homeostasis in bacteria. Nat Rev Microbiol. 2008; 6:222–233. [PubMed: 18264115]

Zolkipli Z, Pedersen CB, Lamhonwah AM, Gregersen N, Tein I. Vulnerability to oxidative stress in vitro in pathophysiology of mitochondrial short-chain acyl-CoA dehydrogenase deficiency: response to antioxidants. PLoS One. 2011; 6:e17534. [PubMed: 21483766]

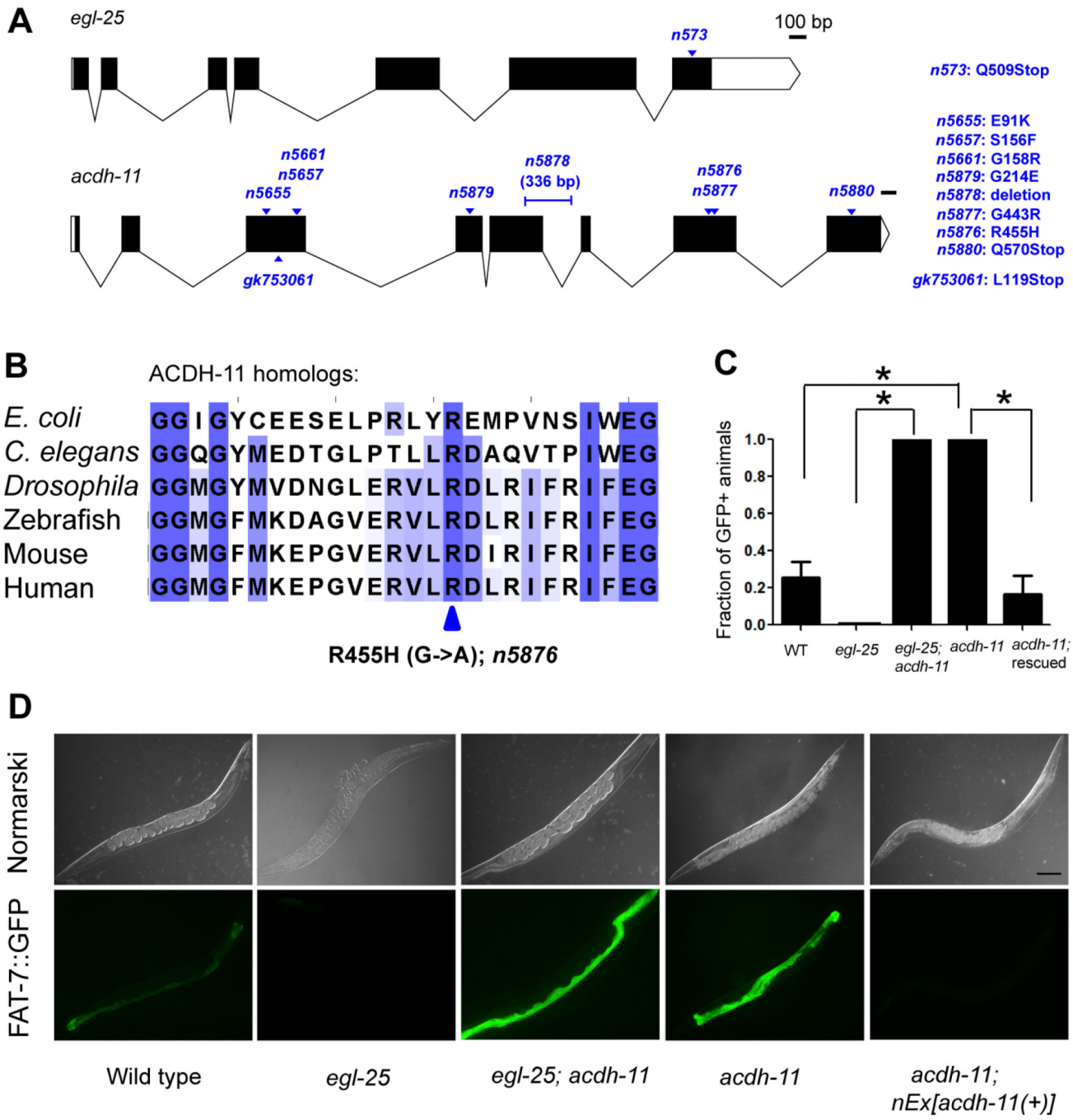

Figure 1. *acdh-11* regulates *fat-7* expression

(A) Schematic of *egl-25* and *acdh-11* gene structures. Shown are *egl-25(n573)*, *acdh-11(gk753061)* and another eight *acdh-11* mutations isolated from *egl-25(n573)* suppressor screens. Both *n573* and *n5880* are ochre (CAA-to-TAA) mutations and *gk753061* is an amber (TTG-to-TAG) mutation. **(B)** Sequence alignments of ACDH-11 homologs from *Escherichia coli* (AidB), *Drosophila melanogaster* (CG7461), *Danio rerio* (Acadvl), *Mus musculus* (Acadvl) and *Homo sapiens* (ACADVL). For clarity, only the regions corresponding to that surrounding amino acid residue R455, which is disrupted by the

acdh-11 mutation *n5876*, are shown. The three shades of blue indicate the degree of amino acid identity (deep blue > 80 %; blue > 60 %; light blue > 40%). Arrow indicates the completely conserved R455 residue, which is disrupted by the *acdh-11(n5876)* mutation. **(C)** Fractions of animals expressing FAT-7::GFP at 20°C as scored visually. $p < 0.01$ (n = 100 for each of five independent experiments). **(D)** EGL-25 and ACDH-11 antagonistically regulate the abundance of the *nIs590[*$P_{fat\text{-}7}$*::fat-7::GFP]* reporter (FAT-7::GFP). Representative Nomarski and GFP fluorescence micrographs are shown of *C. elegans* adults of the genotypes indicated and grown at 20°C. Alleles used were: *egl-25(n573)*, *egl-25(n573); acdh-11(n5655)* and *acdh-11(n5878)*.

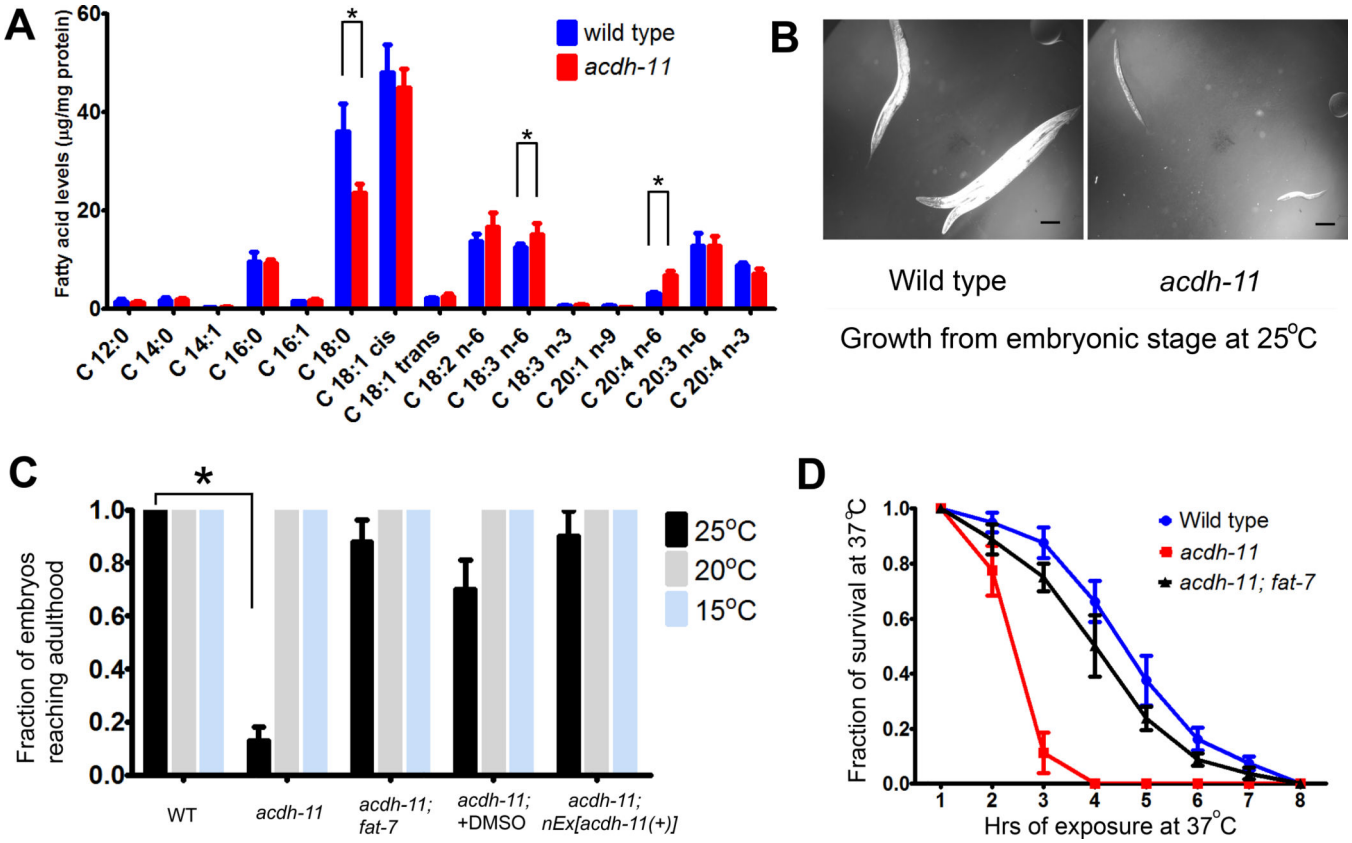

Figure 2. ACDH-11 regulates lipid desaturation and promotes *C. elegans* survival at high temperature

(A) LC-MS profiling of fatty acids extracted from young adult *C. elegans* populations of the wild type and *acdh-11(gk753061)* null mutants. Fatty acids are indicated in the form C:D, where C is the number of carbon atoms in the fatty acid and D is the number of double bonds in the fatty acid. Fatty acid levels were normalized to total protein levels in the wild type and *acdh-11* mutants ($p < 0.01$ from four independent samples for each genotype). **(B)** Bright-field images showing the arrest of larval development of *acdh-11*(*gk753061*) null mutants but not of wild-type animals grown at 25°C. Bleach-synchronized embryos were grown for 4 days at 25°C. **(C)** Fractions of embryos of indicated genotypes or treatment that developed to adulthood at 25°C (under the same conditions as in **B**). $p < 0.01$ ($n = 20$ for each of four independent experiments). **(D)** Fractions of adults that survived 37°C heat stress after shifting animals (24 hrs post-L4) from 15°C to 37°C. After 24 hrs recovery at 15°C, animals without pumping and responses to repeated touch were considered dead and counted for quantification. Error bars, standard deviations ($n = 50$ for each of four independent experiments). Statistical details in Supplemental Information. Scale bars, 100 µm.

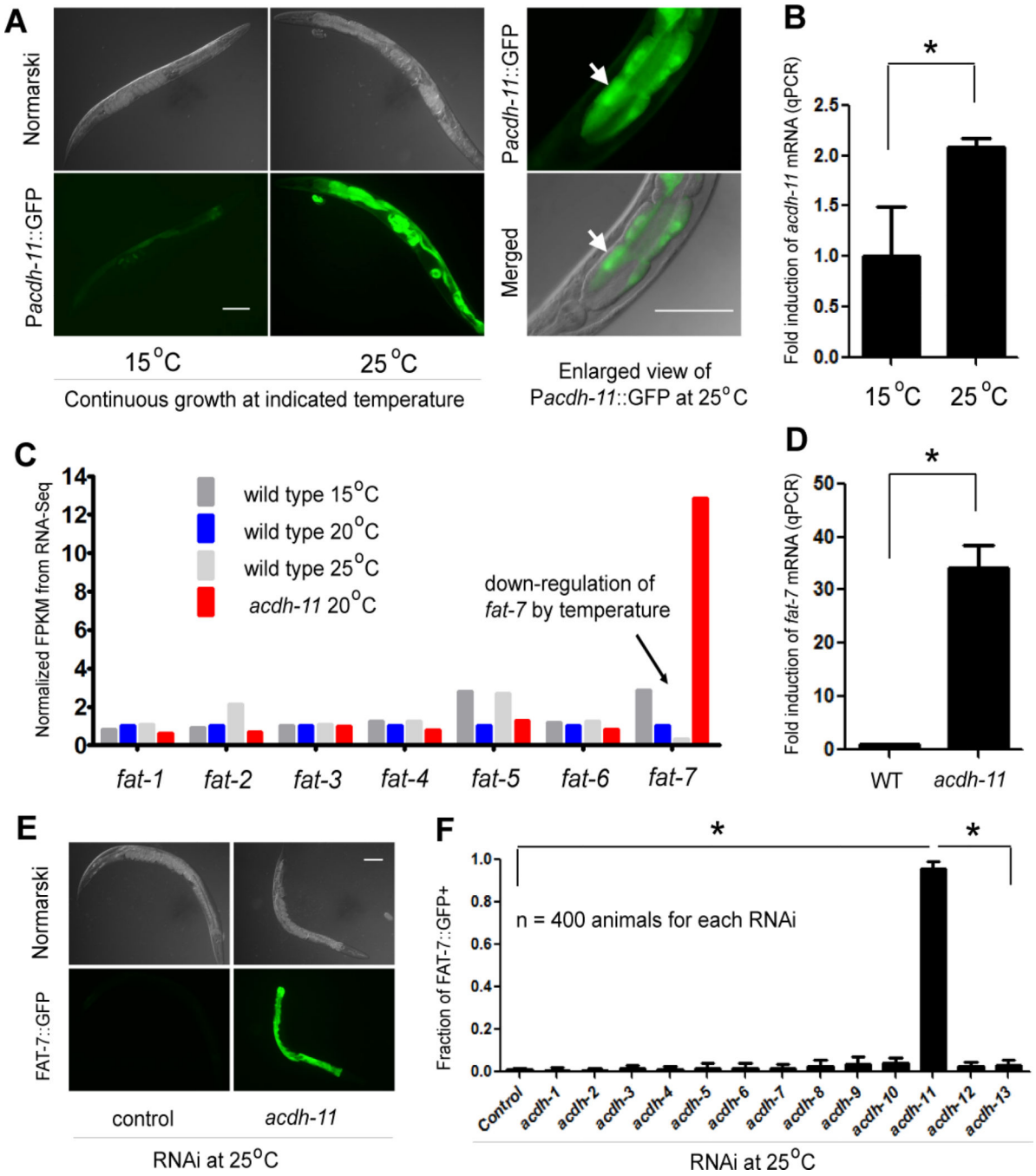

Figure 3. Temperature up-regulates *acdh-11*, causing down-regulation of *fat-7* expression

(A) Representative Nomarski and GFP fluorescence micrographs of wild-type transgenic animals with *nIs677[P$_{acdh-11}$::GFP]* (left), the expression of which is up-regulated by high temperature at 25°C. A high-magnification view of another animal (right) shows GFP predominantly in intestinal cells (arrows). Scale bars, 100 μm. **(B)** qPCR results showing that endogenous *acdh-11* is transcriptionally up-regulated at 25°C. $p < 0.01$ (n = 4 for each genotype). **(C)** RNA-Seq quantification of the expression levels at 15°C, 20°C, and 25°C (normalized to levels at 20°C) of genes encoding all seven *C. elegans* lipid desaturases (*fat-1*

to *fat-7*). Arrow indicates down-regulation of *fat-7* expression by temperature. FPKM, fragments per kilobase of exon per million fragments mapped. **(D)** qPCR quantification showing *fat-7* expression levels in wild-type animals and *acdh-11* mutants. $p < 0.01$ ($n = 4$ for each genotype). **(E)** Representative Nomarski and GFP fluorescence micrographs of wild-type *nIs590* transgenic animals showing that RNAi against *acdh-11* induces FAT-7::GFP expression at 25°C. Scale bars, 100 μm. **(F)** RNAi against all *acdh* gene family members showing that *acdh-11* was specifically required for down-regulating FAT-7 abundance at 25°C. $p < 0.01$ ($n = 100$ for each of four independent experiments).

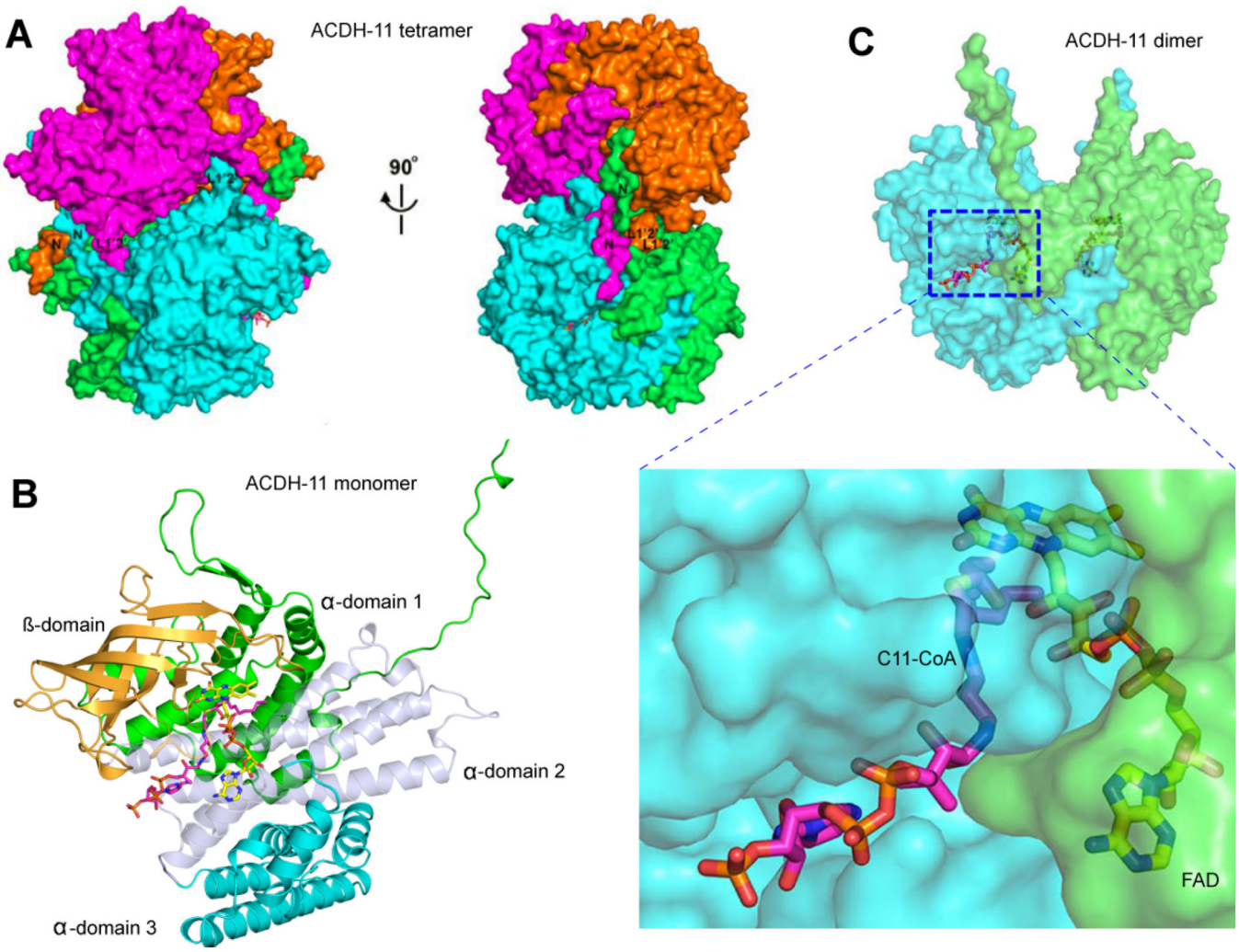

Figure 4. Structure of ACDH-11 showing its binding to the fatty acid C11-CoA

(A) Surface representation of ACDH-11 tetramers showing a dimer of dimers: green-cyan and magenta-orange. For each subunit, the N-terminal loop and the L1'2' loop are shown to form the dimer-dimer interface. **(B)** Ribbon representation of an ACDH-11 monomer showing four domains (α-domain 1, 2, 3 and β-domain). **(C)** Surface representation of an ACDH-11 dimer with an enlarged view of the ligand-binding cavity bound to C11-CoA. FAD, the enzymatic co-factor present in the crystal, is also shown and labeled.

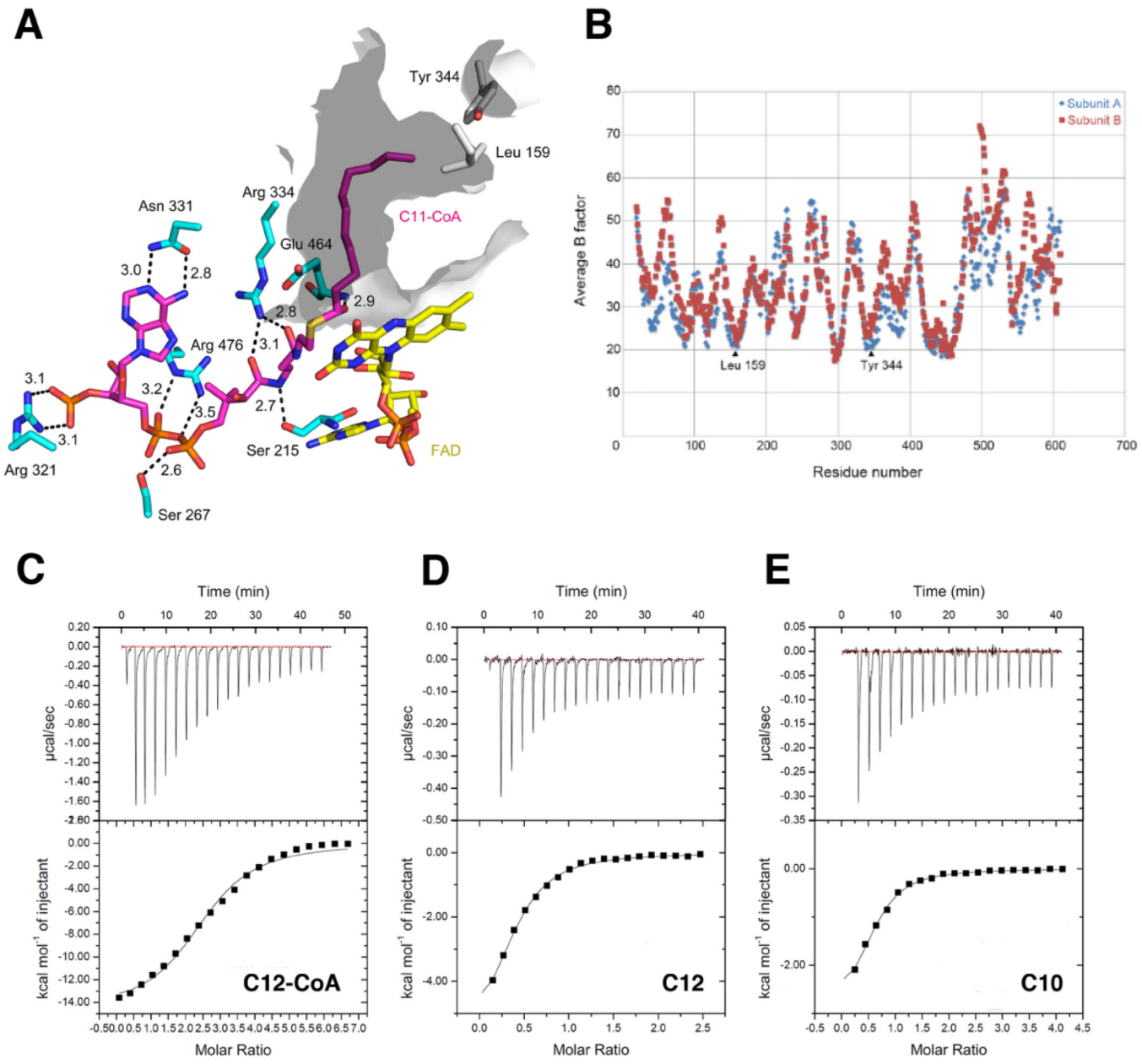

Figure 5. Affinity and selectivity of ACDH-11 binding to acyl-CoA fatty acids

(A) Diagram of C11-CoA interactions with ACDH-11. Arg 321, Asn 331 and Arg 476 form six hydrogen bonds with the CoA moiety; these six bonds are not in other ACDH structures (see Figures S5 and S6). The hydrogen bonds formed by Ser 215, Ser 267, and Arg 334, which are found in SCAD or MCAD (see Figure S6), are also shown. The carbonyl oxygen of the thioester of C11-CoA is hydrogen-bonded with the amino nitrogen of Glu 464, a conserved catalytic residue in ACDHs, indicating a sandwich-like conformation comprising Glu 464, the thioester carbonyl, and the flavin ring. The cavity (grey) depth is limited by Tyr 344 and Leu 159. **(B)** Plot of Temperature-B factor vs. residue number of ACDH-11 showing that both Leu 159 and Tyr 344 have low Temperature B-factors and indicating the low mobility of these two residues. **(C), (D) and (E)** Isothermal titration calorimetry (ITC)

measurements of C12-CoA (C), C12 (D) and C10 (E) binding strengths to ACDH-11. The profiles of the ITC binding data with the baseline subtracted are shown at the top. The peak-integrated and concentration-normalized enthalpy changes vs. the molar ratios of ligands over the ACDH-11 protein are plotted at the bottom.

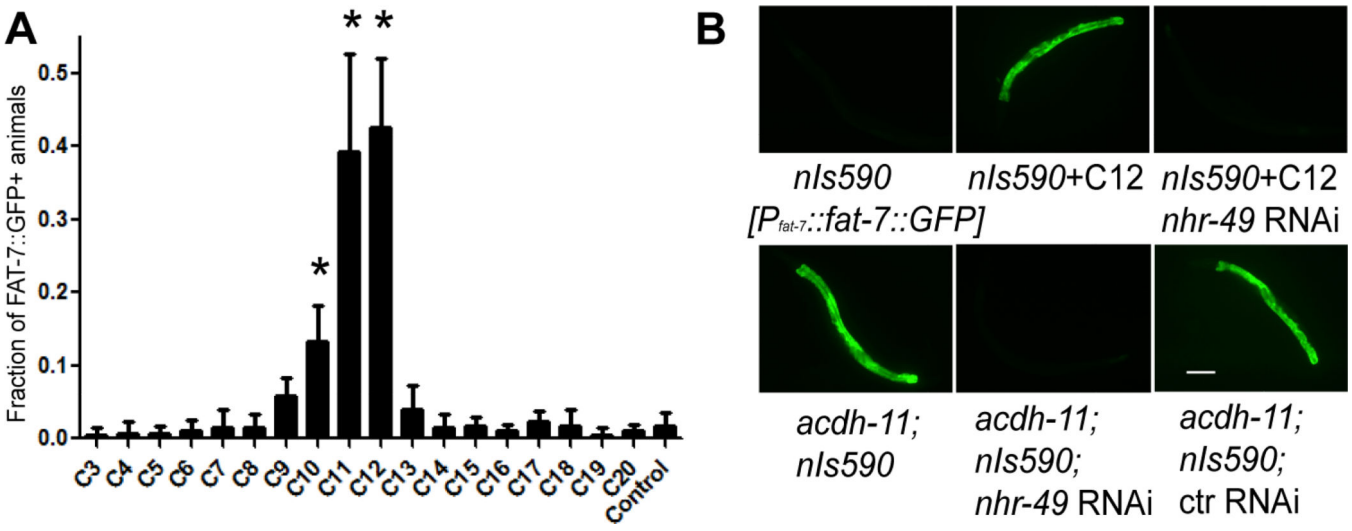

Figure 6. ACDH-11 acts through a fatty acid-mediated transcriptional pathway

(A) Fractions of otherwise wild-type adults carrying the $P_{fat\text{-}7}$*::fat-7::GFP* reporter *nIs590* in which this reporter was activated by various fatty acids. Control, animals treated with only the fatty acid-salt solvent M9 buffer. $p < 0.01$ ($n = 100$ for each of four independent experiments). **(B)** Representative Nomarski and GFP fluorescence micrographs of wild-type transgenic adults showing that RNAi against *nhr-49* blocks activation of *nIs590* reporters by C11/C12 or *acdh-11* mutations. Control, animals with an RNAi vector L4440. Scale bar, 100 μm.

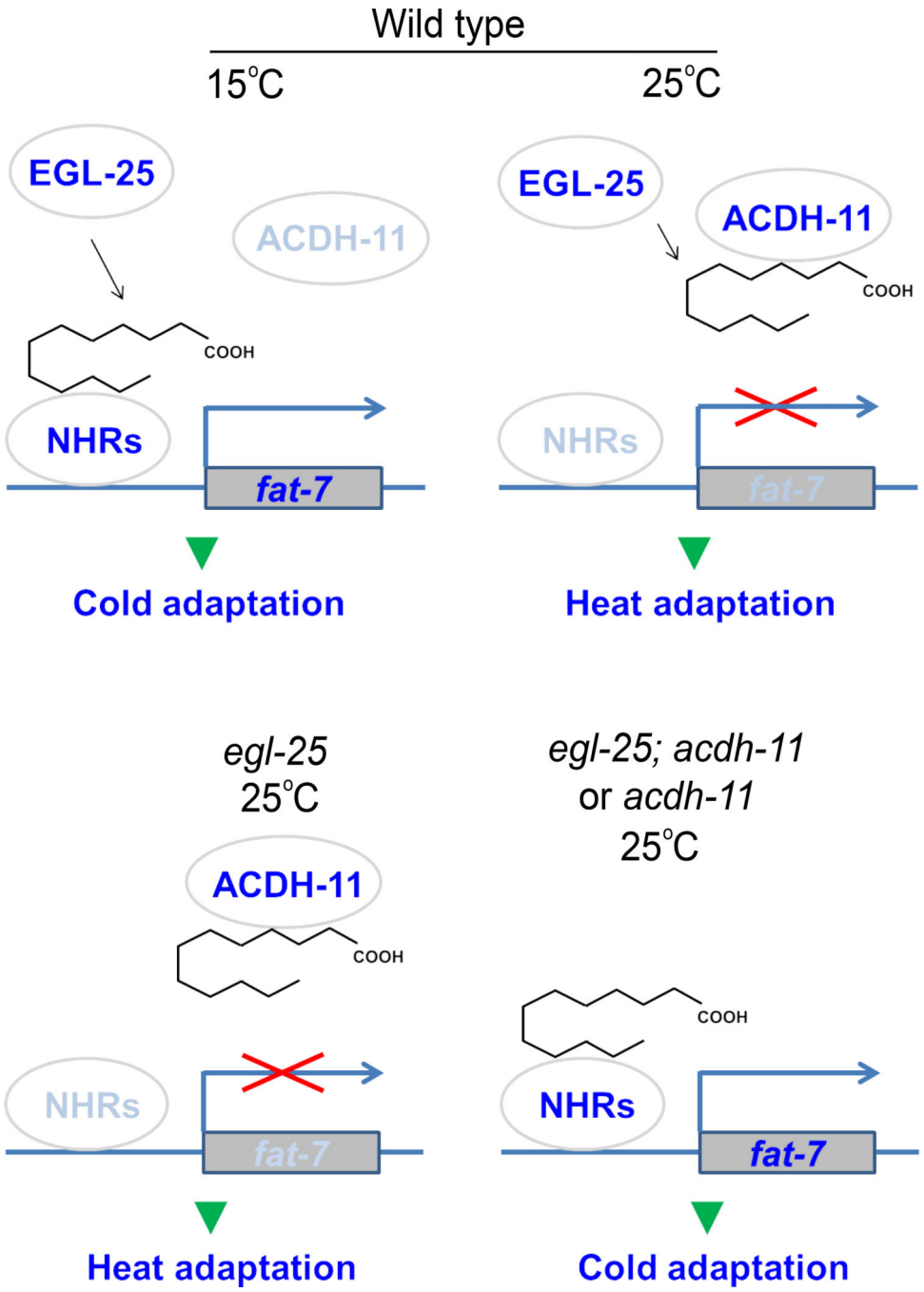

Figure 7. Model for ACDH-11 function

Model showing proposed mechanism for how the ACDH-11 pathway mediates C11/C12 fatty acid signaling and heat adaptation. Heat up-regulates ACDH-11, which prevents C11/C12 from activating NHRs and *fat-7* expression, leading to low levels of membrane lipid desaturation and reduced membrane fluidity for adaptation to heat (see text for details). Light blue indicates low protein activity or a low level of protein abundance. 15°C and 25°C represent low and high temperatures, respectively.